Sequentially linear continuum model for concrete fracture

J.G.Rots
Faculty of Architecture, Delft University of Technology, also TNO Building and Construction Research, Delft, The Netherlands

ABSTRACT: A sequentially linear continuum model for concrete fracture is proposed. The model approximates the tensile softening stress-strain curve as a saw-tooth diagram. After a linear analysis, the critical element, i.e. the element for which the stress is most close to the current peak in the saw-tooth diagram, is traced. Next, the stiffness of that element is reduced and the process is repeated. The sequence of critical states governs the global force-displacement diagram. The elements with reduced stiffness reveal the cracked areas. In fact, the elements are removed in a stepwise manner. The definition of the envelope of the saw-tooth curve uses the notions of fracture energy, tensile strength and crack band width. A notched beam is analysed. Mesh-objectivity can be achieved by adapting both the strength peaks of the saw-tooth diagram as well as the ultimate strain of the diagram to the element dimensions. The potential of the model for large-scale fracture analysis is demonstrated. The very sharp snap-backs associated with brittle fracture of an unreinforced masonry facade automatically come out with sequentially linear analysis, whereas nonlinear analysis of the facade using smeared or discrete crack models show substantial difficulties despite the use of arc-length schemes.

1 INSPIRATION FOR THIS STUDY

1.1 *Settlement damage in large-scale masonry facade*

The fracture model proposed in this paper was inspired by practice-oriented research on settlement damage for masonry structures. Underneath the historical center of Amsterdam a bored tunnel is being planned. The boring of tunnels in soft soil leads to settlements of the soil above the tunnel. These settlements may cause cracking in the existing buildings that are located in the settlement trough area. Fracture mechanics studies are helpful to perform risk analyses and to design mitigating measures. Figs. 1-3 summarize results by Rots (2000). The facade represents three house units with a length of 20.4 m and height 15.5 m. Please note that these dimensions are no less than 150 to 200 times larger than the dimensions of popular notched laboratory beams that usually have a height of approximately 100 mm. First, the facade is subjected to dead load which leads to vertical pre-compression in the masonry. Subsequently, a settlement trough in the form of a Gauss curve is imposed which is incremented until and beyond fracture. The settlement trough leads to bending and shear and superposes tensile stresses to the existing pre-compression, which may

lead to cracking. The aim is to predict (post-peak) crack widths as this is the main damage process that governs the risk. Fig. 1 shows the results for a displacement controlled smeared crack analysis and for an arc-length controlled discrete crack analysis, in terms of the angular distortion, which is related to the magnitude of the settlement trough, versus the maximum crack width in the facade. Fig. 3 shows the deformed mesh for the smeared crack analysis. For the discrete crack analysis, interface elements were predefined at the vertical line where localization was found in the smeared crack analysis. For details of all parameters etc., the reader is referred to Rots (2000). Here, we only display the results, because it is a good illustration of the fact that the behavior is extremely brittle. The large scale in combination with the relatively low fracture energy of masonry leads to a very sharp snap-back in the angular distortion versus crack width diagram of Fig. 1. Only with discrete cracking, this snap-back could be followed partially, by switching between various indirect control parameters (de Borst 1987) over the most active separation node-set of the interface elements. However, the crack has to snap four times, from window to window in the vertical direction, ending up at the top. This saw-tooth four-step nested path could not be traced completely, and sometimes 'luckily' a rigorous jump to another tooth was found,
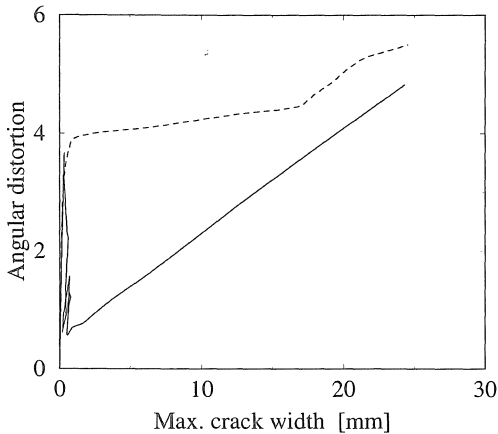
Figure 1. Angular distortion vs. maximum crack width in masonry façade subjected to settlement trough. Smeared (dashed) and discrete crack (drawn) anaysis.
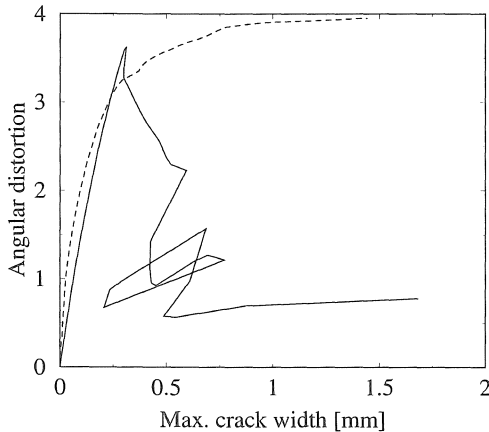

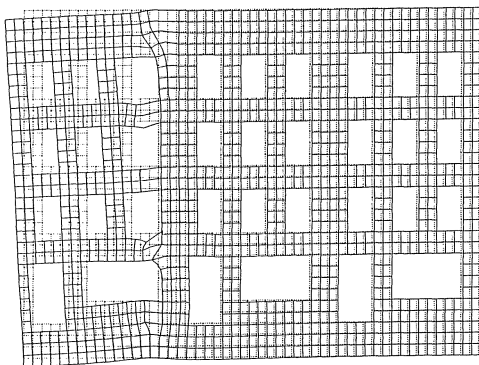Figure 2. Zoom-in of snap-back path in Fig. 1.

Figure 3. Deformed mesh of masonry façade subjected to settlement trough, smeared crack analysis.

see the zoomed-in graph in Fig. 2. Alano & Crisfield (2001) report similar irregular behavior for different applications. After the difficult regime, the discrete crack analysis produced a rising curve again, corresponding to a fully broken facade.

This second branch makes it possible to find the post-peak crack width, which suddenly jumps from approximately 0.5 mm at peak to 18 mm after fracture completion. The discrete crack path was converged. With the smeared crack analysis, no convergence could be found near and beyond peak. Use of a tangent stiffness scheme could not be maintained, while arc-length methods failed, independent whether a decomposed strain based crack model (e.g. Rots 1993), a total strain based crack model (Feenstra et al. 1998) or a Rankine plasticity based crack model (Feenstra & De Borst 1995) was adopted. Fig. 1 shows a rough displacement controlled 'push-through' analysis whereby the secondary branch shows unconverged states. The very brittle response is jumped over and significant stress-locking was observed. The irregular snap-regime of Fig. 2 gave rise to the idea of sequentially linear analysis where the local peaks emerge automatically rather than delicately trying to pass them using arc-length procedures in nonlinear analysis.

1.2 *Lattice models*

Secondly, inspiration came from lattice models, e.g. Schlangen & Van Mier (1992) and Beranek & Hobbelman (1995). In these publications, much emphasis is placed on the imitation of the continuum by a lattice. However, it is stated here that the charm of lattice models is probably not so much the replacement of the continuum by a lattice, but rather the fact that lattice models adopt sequentially linear techniques, so that notions like iteration, spurious behavior and divergence do not appear in the vocabulary. After a linear analysis, the most critical beam element of a lattice is traced and subsequently removed, after which the next linear analysis is carried out and the process is repeated. Problems under study are the proper definition of the lattice structure and the selection of stiffness and strength properties for the lattice elements, which asks for further input from micro-mechanics observations. Furthermore, systematic studies of mesh objectivity (or possibly in-objectivity because of the elastic-brittle characteristics) do not seem to have received much attention for lattice models. In the author's opinion, a scientific debate might be started whether it is really necessary to mimic the continuum by a lattice. The question is whether the charm of sequentially linear analysis can also be gained directly for the continuum, so that the notions of elasticity, strength and fracture energy can be preserved at 'macrolevel'. Together with the motivation in section 1.1, this marked the starting point for the present study.

2 SEQUENTIALLY LINEAR PROCEDURE WITH SAW-TOOTH SOFTENING

2.1 Global procedure

The structure is discretized using standard elastic continuum elements. Young's modulus, Poisson's ratio and a tensile strength are assigned to the elements. Subsequently, the following steps are sequentially carried out:

- Add the external load as a unit load.
- Perform a linear elastic analysis.
- Extract the critical element from the results. The critical element is the element for which the principal tensile stress is most close to its current strength. This principal tensile stress criterion is widely accepted in mode-I fracture mechanics of quasi-brittle materials.
- Calculate the critical global load as the unit load times the current strength divided by stress of the critical element.
- Extract also a corresponding global displacement measure, so that later an overall load-displacement curve can be constructed.
- Reduce the stiffness and strength, i.e. Young's modulus E and tensile strength f_t of the critical element, according to a saw-tooth tensile softening stress strain curve as described in the next section.
- Repeat the previous steps for the new configuration, i.e. re-run a linear analysis for the structure in which E and f_t of the previous critical element are reduced.
- .... Repeat again, etc. ....
- Construct the overall load-displacement curve by connecting all load-displacement sets consecutively found in the above steps.
- Plot deformed meshes. These plots reveal the fracture localization because the series of critical weakened elements will display the largest strains, representing crack width.

2.2 Saw-tooth softening model via stepwise reduction of Young's modulus

The outcome of the above scheme heavily depends on the way in which the stiffness and strength of the critical elements are progressively reduced. This constitutes the essence of the model. A very rough method would be to reduce E to zero immediately after the first, initial strength is reached. This elastic perfectly brittle approach, however, is likely to be mesh dependent as it will not yield the correct energy consumption upon mesh refinement (Bazant and Cedolin 1979). In this study, the consecutive strength and stiffness reduction is based upon the concept of tensile strain softening, which is fairly

accepted in the field of fracture mechanics of concrete (Bazant and Oh, 1983).

The tensile softening stress-strain curve is defined by Young's modulus E, the tensile strength f_t, the shape of the diagram, e.g. a linear or exponential diagram, and the area under the diagram. The area under the diagram represents the fracture energy G_f divided by the crack band width h, which is a discretisation parameter associated with the size, orientation and integration scheme of the finite element. Although there is some size-dependence, the fracture energy can be considered to be a material property. This softening model usually governs nonlinear constitutive behaviour in an incremental-iterative strategy. Please note that here we adopt the curve only as a 'mother' or envelope curve that determines the consecutive strength reduction in sequentially linear analysis. This differs also from a previous study in which element removal was combined with nonlinear analysis (Rots 1992). In the present study, attention is confined to a linear softening diagram, but extension to any other shape of the diagram is possible. For a linear softening diagram, the ultimate strain ε_u of the diagram reads:

$$\varepsilon_u = (2 \, G_f \,) / (f_t \, h) \qquad (1)$$

In a sequentially linear strategy, the softening diagram can be imitated by consecutively reducing Young's modulus as well as the strength. Young's modulus can e.g. be reduced according to:

$$E_i = E_{i-1} / a \qquad \text{for } i = 1 \text{ to } n \qquad (2)$$

with i denoting the current stage in the saw-tooth diagram, i-1 denoting the previous stage in the saw-tooth diagram and a being a constant. When a is taken as 2, Young's modulus of a critical element is reduced by a factor 2 compared to the previous state. n denotes the amount of reductions that is applied in total for an element. When an element has been critical n times, it is removed completely in the next step. This complete removal can be done explicitly so that 'a hole in the mesh' occurs for full cracks, or it can be approximated by maintaining the element but giving it a very low residual Young's modulus for reasons of computational convenience (e.g. 10^{-6} times the initial Young's modulus). The reduced strength f_{ti} corresponding to the reduced Young's modulus E_i is taken in accordance with the envelope softening stress-strain curve:

$$f_{ti} = \varepsilon_u E_i (D / (E_i + D)) \qquad (3)$$

with

$$E_i = E / (a^i) \qquad (4)$$

and

$$D = f_t / (\varepsilon_u - (f_t / E)) \qquad (5)$$

being the tangent to the tensile stress-strain softening curve. Note that this is the softening curve in terms of stress versus *total* strain, i.e. the sum of elastic strain and crack strain of an imagined cracked continuum. The diagram includes the initial rising branch, which is steep compared to the downward slope in case of small-scale elements (small crack band width) and/or high fracture energy. As an example, Fig. 4 shows the envelope softening curve and the corresponding saw-tooth curve for an initial Young's modulus E of 38000 N/mm^2, initial tensile strength f_t of 3 N/mm^2, fracture energy G_f of 0.06 N/mm, crack band width h of 5 mm, factor a equal to 2 and number of reductions n equal to 10.
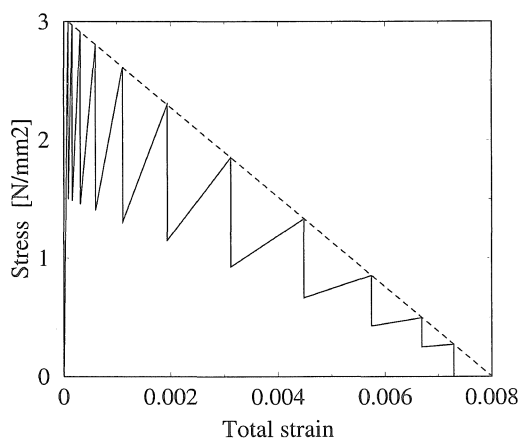

Figure 4. Envelope softening stress-strain diagram (dashed) and saw-tooth approximation (drawn).

Strictly speaking, the sequentially linear approach corresponds to a set of unconnected lines of different slope, starting from the origin up to the current strength. For reasons of presentation, the lines have been connected into one discontinuous curve, by letting the stress drop vertically from the peaks to a residual level at which the new rising branch of reduced slope passes.

The model is simple. It always provides a solution, as ill-conditioning or divergence does not appear in sequentially linear analysis. A physical explanation to the model is that fracture is a gradual separation process whereby the net cross section that connects material, and thus the stiffness, is gradually reduced. An advantage of the model is that the regular notions of fracture mechanics, like the principal tensile stress criterion, the envelope strength and fracture energy are maintained which helps in reaching realistic energy consumption and toughness as observed in experiments.

The model has been elaborated here for continuum crack methods, using softening stress-strain curves. Sequentially linear saw-tooth approaches can also be employed for discrete crack methods with stress-relative displacement curves in interface elements or embedded representations.

Unloading of softening zones is possible and inherently of the secant type, because of the reduction of elasticity.

2.3 *Alternative definition of saw-tooth diagram*

In the previous section, the starting point for defining the saw-tooth diagram was a consecutive reduction of Young's modulus via the factor a while the corresponding reduced strength was subsequently determined from the envelope curve according to (3). In first trials of the model, the starting point was taken alternatively by reducing the strength from f_t to zero in n steps, while the corresponding reduced Young's modulus was subsequently computed from the envelope curve. The decreasing line of the envelope curve is in fact split into n equidistant portions. When n is assumed to be 10 and when the element is critical for the first time, the strength is reduced to 90% of the original strength. When it is critical for the second time, the strength is reduced to 80% of the original strength, etc. The resulting saw-tooth diagram for this alternative approach is depicted in Fig. 5, using the same parameters as subject to Fig. 4. Other alternative ways of stepwise reduction might be used as well.
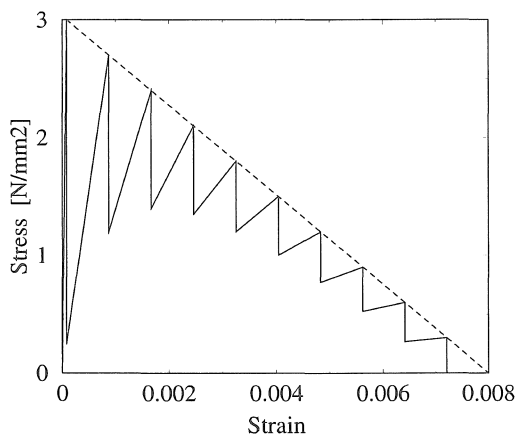

Figure 5. Envelope softening stress-strain diagram (dashed) and alternative saw-tooth approximation (drawn).

3 ANALYSIS OF NOTCHED BEAM

3.1 Geometry and meshes

A symmetric notched beam of total length 500 mm, span 450 mm, height 100mm, thickness 50 mm and notch depth 10 mm was selected for analysis. The distance between the loading points in the symmetric four-point loading scheme is 150 mm. In an earlier study (Rots 1993) this beam served the purpose of illustrating stress-locking for smeared crack models and prevention thereof via isotropic damage formulations. In the present study, on purpose a regular straight mesh was adopted, so that the solution is not affected by any disturbing effect due to zig-zag crack band paths. Four different meshes were used, referred to as coarse, medium, fine and very fine respectively. These meshes have a symmetric center crack band of 20 mm, 10 mm, 5 mm and 2.5 mm width respectively. The element height for the central elements was taken the same as the element width, so that the amount of center elements over the depth of the beam amounts to 5, 10, 20 and 40 respectively. The ultimate strain ε_u of the envelope input curve was adapted to h according to Eq. (1). Four-node linear elements were used. These were integrated using a two by two Gaussian scheme, except for the elements in the center band which were integrated using a single center-point integration. This means that, if an integration point of an element in this center band reaches a local peak in the sawtooth curve, Young's modulus of the entire element can be reduced. The meshes are depicted in Fig. 6.
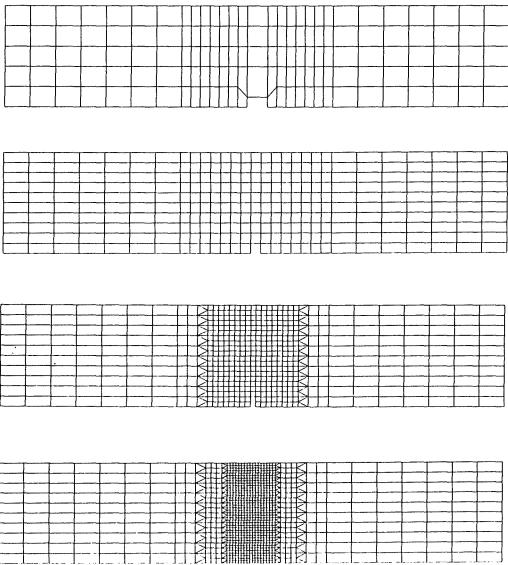

Figure 6. Coarse, medium, fine and very fine mesh for mode-I fracture analysis of notched beam.

The material parameters are the same as mentioned in section 2 for defining Figs. 4 and 5. Poisson's ratio was taken as 0.2. The model of Fig. 4 was adopted. The factor a in Eq. (2) was taken as 2. The factor n was taken as 10, i.e. the stiffness of an element can be reduced 10 times according to Eq. (2), assuming the element becomes 10 times critical in a global sense. Beyond that, the element is removed.

3.2 Results

Figs. 7 to 10 show the results for the four meshes in terms of the total load (sum of the two loads) versus displacement at the loading points. The curves are constructed by connecting the critical loads and the corresponding displacements for all linear analyses that have been executed sequentially. As a comparison, the reference curve (see also Rots 1993) from a nonlinear softening analysis with the same parameters is included in the graphs.
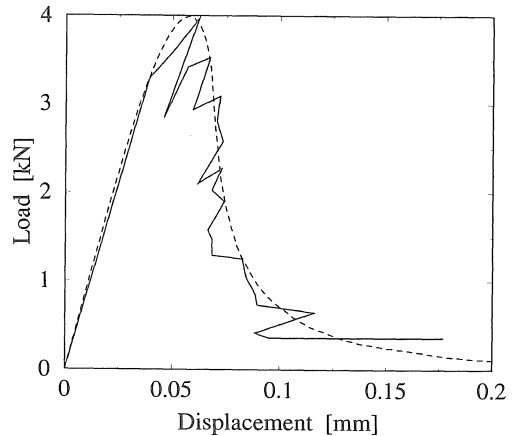

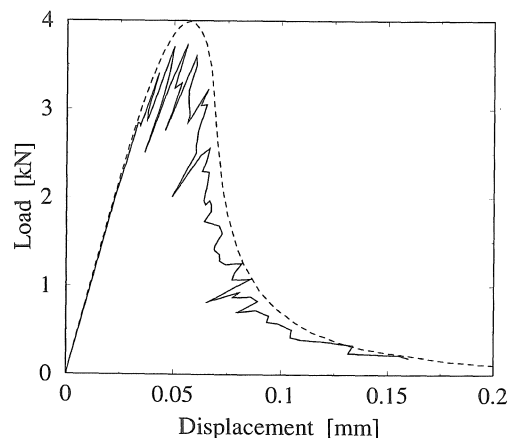Figure 7. Load-displacement curve, coarse mesh.

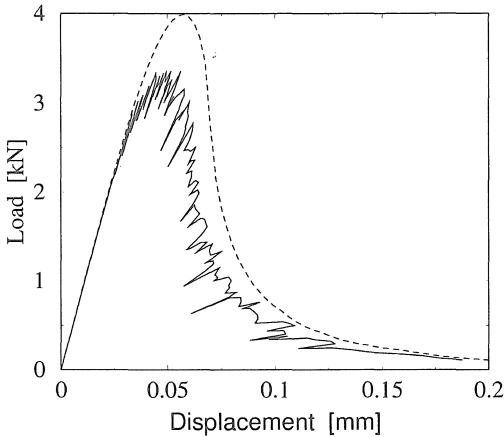Figure 8. Load-displacement curve, medium mesh.
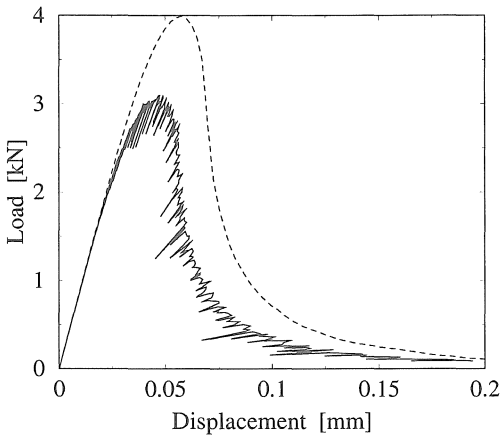
Figure 9. Load-displacement curve, fine mesh.

Figure 10. Load-displacement curve, very fine mesh.

This reference curve appeared to be almost identical for all meshes, except for the coarse mesh where a minor deviation near peak occurred.

For all meshes, the load-displacement curve from sequentially linear analysis is irregular. This is because the process of elements becoming critical is discontinuous. If two elements have almost the same ratio of stress versus current strength, still the most critical one is selected first, but in the next step the other one will fail very soon, maybe at a lower load and lower displacement than in the previous step. This behavior is known also from sequentially linear analysis on lattices. In the present study, the irregular saw-tooth response at global level can be interpreted as the global pendant of the saw-tooth input at local level.

With increasing mesh fineness, the curves become smoother. Surprisingly, the envelope of the curve for the coarse mesh appears to resemble the

reference curve most closely, both in terms of the maximum load and post-peak toughness. Please note that the model is especially derived with a view towards large-scale brittle fracture analysis, i.e. large element sizes, which is thus promising. With increasing mesh fineness, however, the peak in the load-displacement behavior becomes lower and lower compared to the correct peak from the nonlinear reference analysis that is to be mimicked. This demonstrates that sequentially linear models are in principle not objective with respect to mesh refinement. This is because increasing mesh fineness leads to sharper stress peaks at the crack band tip, so that the strength at the crack band tip is reached earlier than for a coarse mesh. In fact, a kind of 'zip-fastener' effect is introduced. With a sudden full removal of elements, i.e. a diagram with only one saw-tooth instead of the present ten saw-teeth, this effect would be even more pronounced. That was described already by Bazant & Cedolin (1979).

3.3 Lifting the strength of the saw-tooth diagram

A natural way to circumvent mesh-inobjective results is to enhance the strength with decreasing element size. This counteracts the zip-fastener effect. Precisely speaking, the input envelope curve and saw-tooth curve should be adapted to the mesh in two ways. First, the ultimate *strain* ε_u of the diagram is adapted to the element *width,* which is equal to the crack band width in the present case of a perfectly vertical crack in a perfectly vertically aligned mesh with constant strain in the direction normal to the crack. This is the same procedure as used for crack band modeling in nonlinear analysis. Now, we add the second adaptation, viz. the ultimate *strength* f_t is adapted to the element *height*, which is again equal to the crack band width h in the present case of a perfectly vertical crack in a mesh composed of perfectly vertical square elements. The adjustment of the ultimate strain to the element width, measured in the direction normal to the crack, is a correct way to handle the spreading of a smeared crack. This was checked by running an analysis on a new mesh that was refined only in the vertical direction, but not in the horizontal direction. This yielded identical results.

At present there is no procedure to quantify the amount of strength enhancement needed upon mesh refinement in the crack propagation direction. For the present example a fitting strategy was followed, to gain some insight. For the various meshes, the strength level was raised by trial and error by a factor *b*, until the maximum load and the post-peak behavior of the nonlinear reference analysis was reproduced most accurately. It is mentioned that upon strength enhancement of the peak of the input envelope curve, also the fracture energy of the input envelope curve has been enhanced with the same

836

amount, in order to keep the ultimate strain of the envelope curve the same. For the present case (and only the present case) this led to the following optimal fits:

- Coarse mesh: no strength raise required, b=1.00.
- Medium mesh: required strength raise b=1.10.
- Fine mesh: required strength raise b=1.20.
- Very fine mesh: required strength raise b=1.42.

As an example, Fig. 11 depicts the result for the fine mesh when the strength is raised by a factor 1.20, together with the previous result from Fig. 9 without strength enhancement.
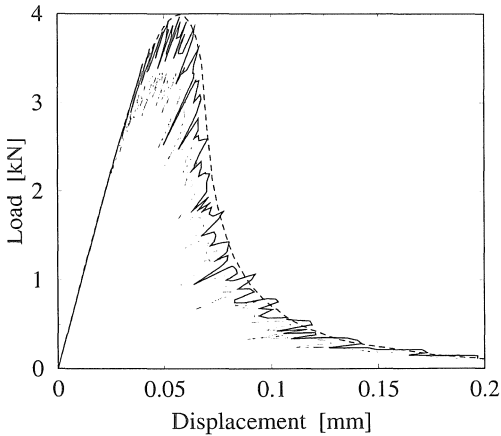

Figure 11. Load-displacement curve, fine mesh, strength and energy enhancement by a factor 1.2 (drawn line), compared with results of Fig. 9 (dashed lines).

The challenge is to derive consistent relationships between the various length scales in a fracture problem on the one hand, e.g. the depth of the structure, the thickness of the structure, the initial notch depth, the fracture process zone length, the so-called brittleness number, and the required strength enhancement on the other hand. Also the material parameters and the factors a and n play a role in this respect. Here, further numerical and theoretical studies are required. The present study only serves the purpose of demonstrating the potential of sequential linear analysis for large-scale structures and/or coarse meshes, but it is frankly admitted that much further research is necessary to get mesh-objective results via a proper rationale. For sequentially linear lattice models, however, a similar statement may be raised, while this has not prevented these models from having become increasingly popular.

3.4 *Alternative saw-tooth model*

Fig. 12 shows a result for the alternative saw-tooth model of Fig. 5, for the coarse mesh, without strength enhancement.
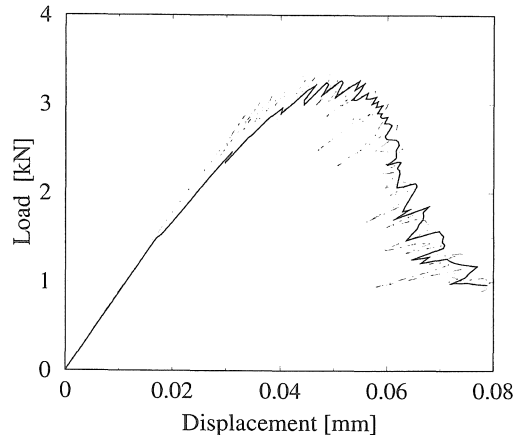

Figure 12. Load-displacement curve, coarse mesh, alternative saw-tooth diagram of Fig. 5 (drawn) compared with previous result of Fig..9 (dashed).

This result shows that the initial pre-peak stiffness of the structure is too low. The fact that the envelope softening diagram is subdivided in, in this case 10, equidistant portions, implies that the first reduction of Young's modulus is much larger than the factor a=2 as assumed in the previous analyses with the diagram of Fig. 4. This explains the flexible pre-peak response. The procedure underlying the saw-tooth diagram of Fig. 4 is to be preferred, although is must be mentioned that this aspect will be related to the absolute dimensions of the crack band width. The present beam is of small-scale laboratory size, giving a low value of h and thus a high ultimate strain compared to the initial elastic strain limit. For large-scale structures of the same material and of the same relative mesh fineness, h becomes much larger and the difference between the input diagrams of Figs. 4 and 5 will be less pronounced.

4 MASONRY FAÇADE

The masonry façade introduced in section 1 was analyzed using the sequentially linear model of Fig. 4. The parameters were taken as: E=3000 N/mm2, f_t=0.6 N/mm2, G_f=0.05 N/mm, crack band width h=225 mm (note: approximately 100 times larger than for the small-scale notched beam), factor a=2, factor n=5. The thickness is 220 mm. For geometry the reader is referred to Rots (2000). A difficulty with this problem is that it involves a non-proportional loading scheme. First, dead weight is added and subsequently the settlement trough. It appears that non-proportional loading for sequentially linear analysis on lattices or other structures has not yet received much attention in literature. A way to solve this is to run sequentially linear analyses for the various load sets in an incremental fashion. First,

the first load set is analysed sequentially linear and the results are frozen. From this frozen situation, the sequentially linear analysis for the second load set is undertaken whereby initial stresses, strains and displacements are accounted for. This process requires the new critical element for the second (or subsequent) load set to be determined again on the basis of the principal stress criterion. The principal stresses now should be derived on the basis of:

$$\sigma_{xx} = \sigma_{xx,0} + \lambda \; \Delta\sigma_{xx}$$
$$\sigma_{yy} = \sigma_{yy,0} + \lambda \; \Delta\sigma_{yy} \qquad (6)$$
$$\sigma_{xy} = \sigma_{xy,0} + \lambda \; \Delta\sigma_{xy}$$

for a plane stress situation, with $_0$ referring to the preceding load set(s) and Δ referring to the increment for the current load set. This is more cumbersome than for the case of the initial stresses being zero. From the resulting equations for the principal stress according to Mohr's circle, λ can be solved directly using e.g. Maple software, or numerically.

In the present study this was not yet implemented. The performance of the model can quite as well be illustrated by using a fictitious, proportional load. Here, a vertical point load at the top of the façade, slightly off-center, was taken as an arbitrary example. Fig. 13 shows the result in terms of the vertical point load versus displacement. Fig. 14 shows the deformed mesh at one of the final steps of the sequentially linear procedure.

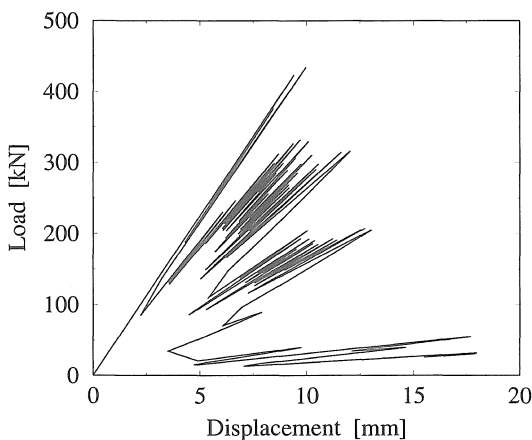Figure 14. Deformed mesh for final stage in Fig. 13.

Figure 13. Load-displacement curve for sequentially linear analysis of masonry façade under point load.

The result reveals the very sharp snap-back behavior, which is found in the sequentially linear fashion without any numerical problems. In the post-peak behavior, we observe four nested snaps, which correspond to the subsequent jumps of the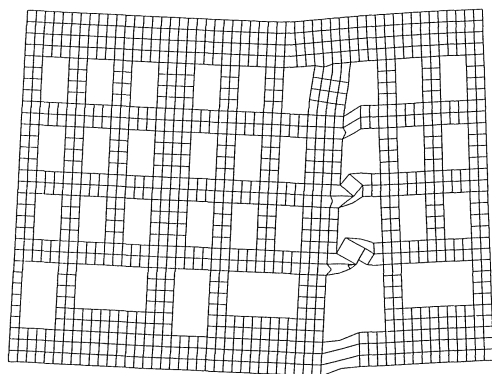 crack from window to window, starting at the bottom and ending at the top of the façade. This is an adequate alternative to the nonlinear analyses summarized in section 1.

A minor aspect is that the present result showed partial stress locking. This was because the mesh consisted of quadratic eight-node elements, integrated by a three by three Gaussian scheme, while the stress at the fifth, central integration point was taken as an element average to be compared with the current strength in the saw-tooth curve. This procedure can be made more accurate by using a mesh of lower order triangular elements, so that a single integration point governs the total element behaviour and false stress transfer is impossible.

5 DISCUSSION

A sequentially linear continuum model for concrete fracture has been proposed. The model approximates an envelope softening stress-strain curve by a saw-tooth diagram. In each linear analysis, a critical element is traced by comparing element stress with current element strength, i.e. with the current peak in the saw-tooth diagram. Next the stiffness and strength of the critical element are reduced according to the subsequent tooth of the diagram, and the process is repeated.

The charm of this model is that words like iteration, ill-conditioning and divergence do not appear in the vocabulary. A notched beam analysis shows the ability of the method to reproduce the behavior of a nonlinear reference analysis on the same parameters. The advantage of the model especially appears in case of brittle, complex snap-back behavior as was illustrated by large-scale analysis of a masonry façade.

Although the model thus has potential, much further research is necessary, especially with regard to mesh objectivity. A method of strength enhancement

in combination with ultimate strain adjustment in order to achieve objective results with respect to mesh refinement was outlined. Also objectivity with regard to mesh orientation should be studied. Here, the strategy followed for nonlinear analysis by Oliver (1989) and Jirasek & Zimmermann (2001) to accurately compute the crack band width and to use a non-local principal stress criterion, can be adopted in the same way for sequentially linear analysis. For triangular meshes, promising results are obtained already for the present local principal stress initiation criterion, as shown in Fig. 15 for the SEN-beam described by Schlangen & Van Mier (1992).
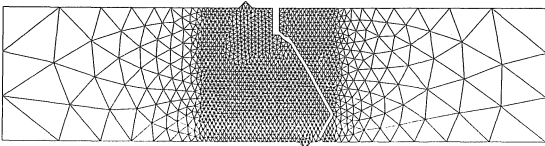

Figure 15. Deformed mesh for sequentially linear analysis of SEN-beam on triangular mesh. A 'hole in the mesh' occurs corresponding to the crack direction in the experiment.

The present formulation of the model is isotropic because Young's modulus is reduced for all directions. Extension of the model to fixed planes of orthotropy is possible, including memory of unloading/reloading and full crack closure and re-opening. An extension of the model to non-proportional loadings has been outlined, which is important in building engineering as vertical dead load is often superimposed by horizontal wind load.

6 ACKNOWLEDGEMENT

REFERENCES

Alfano, G. & Crisfield, M.A. 2001. Finite element interface models for the delamination analysis of laminated composites: mechanical and computational issues. *Int. J. for Numerical Methods in Engineering* 50(7): 1701-1736.

Bazant, Z.P. & Cedolin, L. 1979. Blunt crack band propagation in finite element analysis. ASCE *J. Engineering Mechanics Division* 105(2): 297-315.

Bazant, Z.P. & Oh, B.H. 1983. Crack band theory for fracture of concrete. RILEM *Materials and Structures* 16(93): 155-177.

Beranek, W.J. & Hobbelman, G.J. 1985. 2D and 3D-Modelling of concrete as an assemblage of spheres: revaluation of the failure criterion. In F.H. Wittmann (ed.), *Fracture mechanics of concrete structures; Proc. FRAMCOS*-2: 965-978. Freiburg: Aedificatio.

Borst, R. de. 1987. Computation of post-bifurcation and post-failure behavior of strain-softening solids. *Computers & Structures* 25(2): 211-224.

Feenstra, P.H., Rots, J.G., Arnesen, A., Teigen, J.G. & Hoiseth, K.V. 1998. A 3D constitutive model for concrete based on a co-rotational concept. In R. de Borst et al. (eds.), *Computational modelling of concrete structures; Proc. EURO-C 1998*: 13-22. Rotterdam: Balkema.

Feenstra, P.H. & Borst, R. de. 1995. A plasticity model and algorithm for mode-I cracking in concrete. *Int. J. for Numerical Methods in Engineering* 38: 2509-2530.

Jirasek, M. & Zimmermann, T. 2001. Embedded crack model: II. *Int. J. for Numerical Methods in Engineering* 50(6): 1269-1290.

Oliver, J. 1989. A consistent characteristic length for smeared cracking models. *Int. J. for Numerical Methods in Engineering* 28: 461-474.

Rots, J.G. 1992. Removal of finite elements in smeared crack analysis. In D.R.J. Owen et al. (eds.), *Proc. Third Int. Conf. on Computational Plasticity*: 669-680. Swansea UK: Pineridge press.

Rots, J.G. 1993. The smeared crack model for localized mode-I tensile fracture. In F.H. Wittmann (ed.), *Numerical models for fracture mechanics*: 101-113. Rotterdam: Balkema.

Rots, J.G. 2000. Settlement damage predictions for masonry. In L.G.W. Verhoef and F.H. Wittmann (eds.), *Maintenance and restrengthening of materials and structures - Brick and brickwork, Proc. Int. Workshop on Urban heritage and building maintenance*: 47-62. Freiburg: Aedificatio.

Schlangen, E. & Van Mier, J.G.M. 1992. Experimental and numerical analysis of micro-mechanisms of fracture of cement-based composites. *Cement & Concrete Composites* 14:105-118.